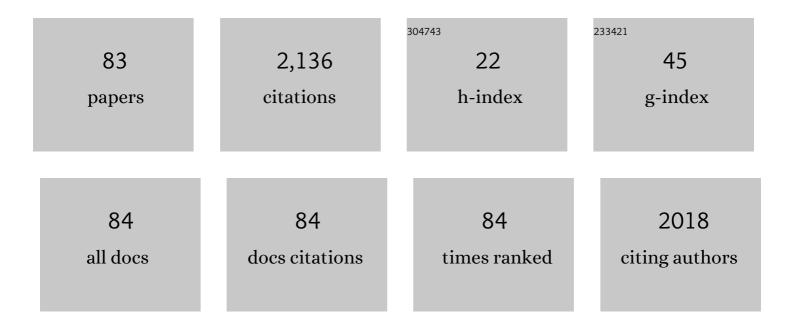
List of Publications by Year in descending order

Source: https://exaly.com/author-pdf/2141943/publications.pdf Version: 2024-02-01



YASHO ANDO

#	Article	IF	CITATIONS
1	Large tunnel magnetoresistance in magnetic tunnel junctions using a Co2MnSi Heusler alloy electrode and a MgO barrier. Applied Physics Letters, 2008, 93, .	3.3	249
2	Half-metallicity and Gilbert damping constant in Co2FexMn1â^'xSi Heusler alloys depending on the film composition. Applied Physics Letters, 2009, 94, .	3.3	214
3	Epitaxial Mn2.5Ga thin films with giant perpendicular magnetic anisotropy for spintronic devices. Applied Physics Letters, 2009, 94, .	3.3	193
4	Tunneling magnetoresistance of magnetic tunnel junctions using perpendicular magnetization L10-CoPt electrodes. Applied Physics Letters, 2008, 92, .	3.3	148
5	Gilbert damping constants of Ta/CoFeB/MgO(Ta) thin films measured by optical detection of precessional magnetization dynamics. Physical Review B, 2014, 89, .	3.2	127
6	Fabrication of Co2MnAl Heusler Alloy Epitaxial Film Using Cr Buffer Layer. Japanese Journal of Applied Physics, 2005, 44, 6535-6537.	1.5	68
7	Fabrication of <i>L</i> 1-MnAl perpendicularly magnetized thin films for perpendicular magnetic tunnel junctions. Journal of Applied Physics, 2012, 111, .	2.5	64
8	Fabrication of magnetic tunnel junctions with a bottom synthetic antiferro-coupled free layers for high sensitive magnetic field sensor devices. Journal of Applied Physics, 2012, 111, .	2.5	55
9	Electrical transport properties of perpendicular magnetized Mn-Ga epitaxial films. Applied Physics Letters, 2010, 96, .	3.3	53
10	Anomalous Hall effect in polycrystalline Mn3Sn thin films. Applied Physics Letters, 2018, 113, .	3.3	50
11	Magnetic damping constant of Co2FeSi Heusler alloy thin film. Journal of Applied Physics, 2007, 101, 09J501.	2.5	49
12	Composition dependence of magnetoresistance effect and its annealing endurance in tunnel junctions having Mn-Ga electrode with high perpendicular magnetic anisotropy. Applied Physics Letters, 2011, 99,	3.3	45
13	Structure, exchange stiffness, and magnetic anisotropy of Co2MnAlxSi1â^'x Heusler compounds. Journal of Applied Physics, 2009, 106, .	2.5	42
14	Spin transfer switching in the nanosecond regime for CoFeB/MgO/CoFeB ferromagnetic tunnel junctions. Journal of Applied Physics, 2008, 103, 103911.	2.5	40
15	Fabrication of L1 ₀ -Ordered MnAl Films for Observation of Tunnel Magnetoresistance Effect. Japanese Journal of Applied Physics, 2013, 52, 063003.	1.5	38
16	Serial MTJ-Based TMR Sensors in Bridge Configuration for Detection of Fractured Steel Bar in Magnetic Flux Leakage Testing. Sensors, 2021, 21, 668.	3.8	36
17	Effect of metallic Mg insertion on the magnetoresistance effect in MgO-based tunnel junctions using <i>D</i> 22-Mn3-Î'Ga perpendicularly magnetized spin polarizer. Journal of Applied Physics, 2011, 110, .	2.5	30
18	Efficiency of ultrafast optically induced spin transfer in Heusler compounds. Physical Review Research, 2020, 2, .	3.6	29

#	Article	lF	CITATIONS
19	Exchange biases of Co, Py, Co40Fe40B20, Co75Fe25, and Co50Fe50 on epitaxial BiFeO3 films prepared by chemical solution deposition. Journal of Applied Physics, 2011, 109, .	2.5	28
20	Influence of <mml:math xmlns:mml="http://www.w3.org/1998/Math/MathML"><mml:mrow><mml:mi>L</mml:mi><mml:msub><mml:n order parameter on Gilbert damping constants for FePd thin films investigated by means of time-resolved magneto-optical Kerr effect. Physical Review B, 2016, 94, .</mml:n </mml:msub></mml:mrow></mml:math 	ın>13.2	l:mŋչ <mml:m< td=""></mml:m<>
21	Ferrimagnetism in epitaxially grown Mn2VAl Heusler alloy investigated by means of soft x-ray magnetic circular dichroism. Applied Physics Letters, 2009, 95, 222503.	3.3	25
22	Spin-dependent transport behavior in C60 and Alq3 based spin valves with a magnetite electrode (invited). Journal of Applied Physics, 2014, 115, .	2.5	25
23	Probing the electronic and spintronic properties of buried interfaces by extremely low energy photoemission spectroscopy. Scientific Reports, 2015, 5, 8537.	3.3	21
24	Tunnel magnetoresistance effect in magnetic tunnel junctions using epitaxial Co2FeSi Heusler alloy electrode. Journal of Applied Physics, 2009, 105, .	2.5	20
25	Low magnetic damping and large negative anisotropic magnetoresistance in half-metallic Co2â^'xMn1+xSi Heusler alloy films grown by molecular beam epitaxy. Applied Physics Letters, 2018, 112, .	3.3	20
26	Quadratic magneto-optical Kerr effect in Co2MnSi. Journal of Applied Physics, 2011, 110, 043904.	2.5	18
27	Evaluation of interlayer exchange coupling in α-Fe(100)/Nd2Fe14B(001) films. Journal of the Korean Physical Society, 2013, 63, 489-492.	0.7	18
28	L1 ₀ -ordered MnAl thin films with high perpendicular magnetic anisotropy. Japanese Journal of Applied Physics, 2017, 56, 0802A2.	1.5	18
29	Reduction in switching current using a low-saturation magnetization Co–Fe–(Cr, V)–B free layer in MgO-based magnetic tunnel junctions. Journal of Applied Physics, 2009, 105, 07D117.	2.5	17
30	Fabrication of MgO-based magnetic tunnel junctions with CoCrPt perpendicularly magnetized electrodes. Journal of Applied Physics, 2009, 105, 07C911.	2.5	16
31	Interface effects on perpendicular magnetic anisotropy for molecular-capped cobalt ultrathin films. Applied Physics Letters, 2011, 99, 162509.	3.3	16
32	Tunneling spectroscopy in CoFeBâ^•MgOâ^•CoFeB magnetic tunnel junctions. Journal of Applied Physics, 2006, 99, 08A905.	2.5	15
33	Improvement of Large Anomalous Hall Effect in Polycrystalline Antiferromagnetic Mn3+x Sn Thin Films. IEEE Transactions on Magnetics, 2019, 55, 1-4.	2.1	15
34	Effect of second-order magnetic anisotropy on nonlinearity of conductance in CoFeB/MgO/CoFeB magnetic tunnel junction for magnetic sensor devices. Scientific Reports, 2019, 9, 17018.	3.3	15
35	Al Aided Noise Processing of Spintronic Based IoT Sensor for Magnetocardiography Application. , 2020, , .		15
36	Fabrication and evaluation of highly c-plane oriented Mn3Sn thin films. AIP Advances, 2020, 10, 015310.	1.3	15

#	Article	IF	CITATIONS
37	Scalp attached tangential magnetoencephalography using tunnel magneto-resistive sensors. Scientific Reports, 2022, 12, 6106.	3.3	15
38	Magnetic Tunnel Junctions With [Co/Pd]-Based Reference Layer and CoFeB Sensing Layer for Magnetic Sensor. IEEE Transactions on Magnetics, 2016, 52, 1-4.	2.1	14
39	Magnetic sensor based on serial magnetic tunnel junctions for highly sensitive detection of surface cracks. Journal of Applied Physics, 2017, 122, .	2.5	14
40	Bias-voltage dependence of magnetoresistance in magnetic tunnel junctions grown on Al2O3 (0001) substrates. Applied Physics Letters, 2005, 86, 102506.	3.3	13
41	Modification of the Interface Nanostructure and Magnetic Properties in Nd-Fe-B Thin Films. Nanoscale Research Letters, 2016, 11, 33.	5.7	12
42	Structural, magnetic, and ferroelectric properties of multiferroic BiFeO3-based composite films with exchange bias. Journal of Applied Physics, 2009, 105, 07D903.	2.5	11
43	Silica coating of Co–Pt alloy nanoparticles prepared in the presence of poly(vinylpyrrolidone). Journal of Nanoparticle Research, 2009, 11, 1787-1794.	1.9	11
44	Fabrication of Multiferroic Co-Substituted BiFeO3 Epitaxial Films on SrTiO3 (100) Substrates by Radio Frequency Magnetron Sputtering. Materials, 2011, 4, 1087-1095.	2.9	11
45	Detection of Small Magnetic Fields Using Serial Magnetic Tunnel Junctions with Various Geometrical Characteristics. Sensors, 2020, 20, 5704.	3.8	11
46	Systematic Investigation on Correlation Between Sensitivity and Nonlinearity in Magnetic Tunnel Junction for Magnetic Sensor. IEEE Transactions on Magnetics, 2015, 51, 1-4.	2.1	10
47	Magnetic Properties of Single Crystalline Co2MnAl Heusler Alloy Thin Films. Journal of Superconductivity and Novel Magnetism, 2012, 25, 2659-2663.	1.8	9
48	Micro-Focused Pulse Laser-Induced Propagating Spin Waves in Permalloy Films With Different Thicknesses. IEEE Transactions on Magnetics, 2017, 53, 1-4.	2.1	9
49	Investigation of a Magnetic Tunnel Junction Based Sensor for the Detection of Defects in Reinforced Concrete at High Lift-Off. Sensors, 2019, 19, 4718.	3.8	9
50	Deep Learning Models for Magnetic Cardiography Edge Sensors Implementing Noise Processing and Diagnostics. IEEE Access, 2022, 10, 2656-2668.	4.2	8
51	Reproducible trajectory on subnanosecond spin-torque magnetization switching under a zero-bias field for MgO-based ferromagnetic tunnel junctions. Applied Physics Letters, 2010, 96, 142502.	3.3	7
52	Influence of diffusion of Fe atoms into the emissive layer of an organic light-emitting device on the luminescence properties. Journal of Applied Physics, 2005, 97, 10D501.	2.5	6
53	Engineered Heusler Ferrimagnets with a Large Perpendicular Magnetic Anisotropy. Materials, 2015, 8, 6531-6542.	2.9	6
54	Controlled growth and magnetic property of a-plane-oriented Mn3Sn thin films. AIP Advances, 2019, 9, 035109.	1.3	5

#	Article	IF	CITATIONS
55	Scaling of quadratic and linear magneto-optic Kerr effect spectra with L21 ordering of Co2MnSi Heusler compound. Applied Physics Letters, 2020, 116, .	3.3	5
56	Tunnel magnetoresistance effect in double magnetic tunnel junctions using half-metallic Heusler alloy electrodes. Journal of Applied Physics, 2009, 105, 07C920.	2.5	4
57	Enhancement of magnetoresistance using CoFe/Ru/CoFe synthetic ferrimagnetic pinned layer in BiFeO3 based spin-valves. Applied Physics Letters, 2012, 101, 072901.	3.3	4
58	Grain-Size-Dependent Low-Temperature Electrical Resistivity of Polycrystalline Co2MnAl Heusler Alloy Thin Films. Journal of Superconductivity and Novel Magnetism, 2017, 30, 1577-1584.	1.8	4
59	Structural and Magnetic Properties in Mn2VAl Full-Heusler Epitaxial Thin Films. IEEE Transactions on Magnetics, 2017, 53, 1-4.	2.1	4
60	Experimental Investigation of the Temperature-Dependent Magnon Density and Its Influence on Studies of Spin-Transfer-Torque-Driven Systems. IEEE Magnetics Letters, 2017, 8, 1-5.	1.1	4
61	Compositional Dependence of Exchange Anisotropy in Pt\$_x\$Mn\$_{100-}\$\$_x\$/Co\$_y\$Fe\$_{100-}\$\$_y\$ Films. IEEE Magnetics Letters, 2019, 10, 1-5.	1.1	4
62	Polycrystalline Co2Fe0.4Mn0.6Si Heusler alloy thin films with high B2 ordering and small magnetic anisotropy for magnetic tunnel junction based sensors. AIP Advances, 2019, 9, 125036.	1.3	4
63	High-Temperature Magnetic Tunnel Junction Magnetometers Based on L1\$_0\$-PtMn Pinned Layer. , 2020, 4, 1-4.		4
64	Large spin signals in <i>n+</i> -Si/MgO/Co2Fe0.4Mn0.6Si lateral spin-valve devices. Journal of Applied Physics, 2020, 127, .	2.5	4
65	Guidelines for attaining optimal soft magnetic properties in FeAlSi films. Applied Physics Letters, 2022, 120, .	3.3	4
66	Structural characterization of epitaxial multiferroic BiFeO3 films grown on SrTiO3 (100) substrates by crystallizing amorphous Bi-Fe-Ox. Journal of the Ceramic Society of Japan, 2010, 118, 648-651.	1.1	3
67	Tunneling magnetoresistance effect in MnGa based perpendicular magnetic tunnel junction with Fe/Co interlayer. Journal of Applied Physics, 2013, 114, 163913.	2.5	3
68	Observation of single-spin transport in an island-shaped CoFeB double magnetic tunnel junction prepared by magnetron sputtering. Philosophical Magazine, 2016, 96, 310-319.	1.6	3
69	Realization of a Spin-Wave Switch Based on the Spin-Transfer-Torque Effect. IEEE Magnetics Letters, 2018, 9, 1-5.	1.1	3
70	Composition dependence of the second-order interfacial magnetic anisotropy for MgO/CoFeB/Ta films. AIP Advances, 2019, 9, 125053.	1.3	3
71	Fabrication of soft-magnetic FeAlSi thin films with nm-order thickness for the free layer of magnetic tunnel junction based sensors. AIP Advances, 2020, 10, .	1.3	3
72	Tunnel magnetoresistance in magnetic tunnel junctions with FeAlSi electrode. AIP Advances, 2021, 11, .	1.3	3

#	Article	IF	CITATIONS
73	Magnetic Properties of Polymer Lb Films Containing Ferrocene Derivatives. Molecular Crystals and Liquid Crystals, 1996, 286, 89-94.	0.3	2
74	Mode change of vortex core oscillation induced by large direct current in 120 nm sized current perpendicular-to-plane giant magnetoresistance devices with a perpendicular polarizer. Applied Physics Letters, 2014, 105, 052407.	3.3	2
75	Epitaxial L10-MnAl Thin Films With High Perpendicular Magnetic Anisotropy and Small Surface Roughness. IEEE Transactions on Magnetics, 2018, 54, 1-4.	2.1	2
76	Controlling domain configuration of the sensing layer for magnetic tunneling junctions by using exchange bias. AIP Advances, 2020, 10, 025119.	1.3	2
77	Observation of Magnetoresistance Effect in \$n\$ -Type Non-Degenerate Germanium With Co2Fe0.4Mn0.6Si Heusler Alloy Electrodes. IEEE Transactions on Magnetics, 2017, 53, 1-4.	2.1	2
78	Interface state and coercivity in Nd-Fe-B/Dy films. Journal of the Korean Physical Society, 2013, 63, 616-619.	0.7	1
79	Penetration depth of transverse spin current in (001)-oriented epitaxial ferromagnetic films. Journal of Magnetism and Magnetic Materials, 2014, 368, 333-337.	2.3	1
80	Half-metallicity and Gilbert damping constant in Co2FexMn1â^'xSi Heusler alloys depending on the film composition. , 0, .		1
81	Dependence of spin-transfer switching characteristics in magnetic tunnel junctions with synthetic free layers on coupling strength. Journal of Applied Physics, 2012, 111, 07C905.	2.5	0
82	Quadratic magnetoelectric effect during field cooling in sputter grown <mml:math xmlns:mml="http://www.w3.org/1998/Math/MathML"> <mml:mrow> <mml:msub> <mml:mi> Cr</mml:mi> <mml:m mathvariant="normal">O <mml:mn> 3</mml:mn> </mml:m </mml:msub> </mml:mrow> films. Physical Review Materials, 2021, 5, .</mml:math 	n>22.4	l:mn>
83	Preparation of Functional Polymer LB film Assemblies. Journal of Japan Oil Chemists' Society, 1998, 47, 323-331,386.	0.3	Ο